LABORATORI NAZIONALI DI FRASCATI
SIS-Pubblicazioni

LNF-01/005 (P)
1 Febbraio 2001

LONGITUDINAL SINGLE-BUNCH INSTABILITIES

Mauro Migliorati, Luigi Palumbo
INFN, Laboratori Nazionali di Frascati, P.O. Box 13, I-00044 Frascati, Italy, and
Università di Roma "LA SAPIENZA", Dipartimento di Energetica

Abstract

After introducing the concepts of longitudinal wakefield and coupling impedance, we review the theory of longitudinal single-bunch collective effects in storage rings. From the Fokker-Planck equation we first derive the stationary solution describing the natural single-bunch regime, and then treat the problem of microwave instability, showing the different approaches used for estimating the threshold current. We end the lecture with the semi-empirical laws that allow us to obtain the single-bunch behavior above threshold, and with a description of the simulation codes that are now reliable tools for investigating all these effects.

PACS:29.20.Dh, 29.27.Bd

Presented at Joint Accelerator School 2000, 3 - 11 July 2000, Russia

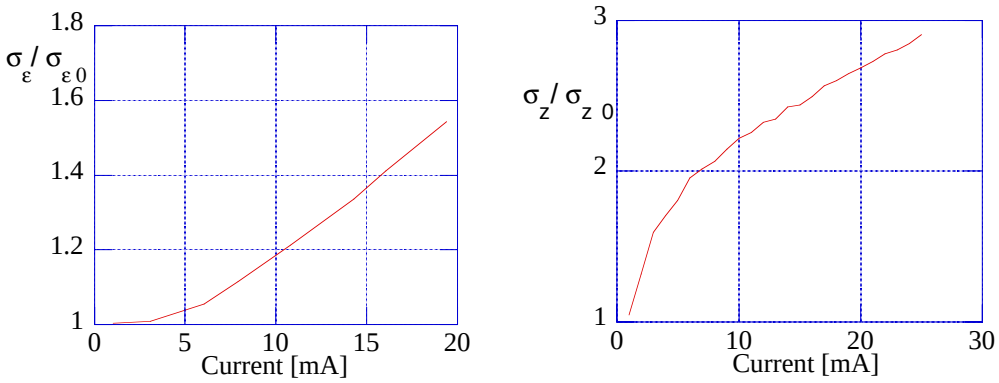

Figure 1: Qualitative behavior of σ_ε and σ_z as a function of current for a generic machine.

1 Observations

If we measure in a circular accelerator the RMS energy spread σ_ε and the RMS bunch length σ_z as a function of the current, parameters of great importance for the machine performance, we obtain qualitatively the behavior plotted in Figure 1.

The energy spread is almost constant up to a threshold current, called the microwave instability threshold, after which it starts to increase with the current according to a given power law (in most cases 1/3 power). The bunch length instead starts to increase from the very beginning, and, after the same threshold current, it grows with the same power law.

Furthermore, it may happen that above the threshold, depending on the wakefields and on the machine parameters, a sawtooth-like behavior is excited (Figure 2).

Although these effects can limit the machine performance, they make the single-bunch dynamics quite attractive from the dynamical point of view. Several physical effects are involved: RF capture, quantum fluctuations, radiation, self-fields interaction, etc. Moreover, this scenario is complicated when nonlinear effects become significant.

In the following sections we will give the basic equations and some models useful for describing the single-bunch dynamics, although a general theory able to predict single-bunch behavior in all its manifestations is still missing.

2 Wakefield and Impedance

2.1 Longitudinal Wake Function

The interaction of a beam with its surroundings[1] is of great importance for the study of beam dynamics since it is responsible of all the collective instabilities. The fields

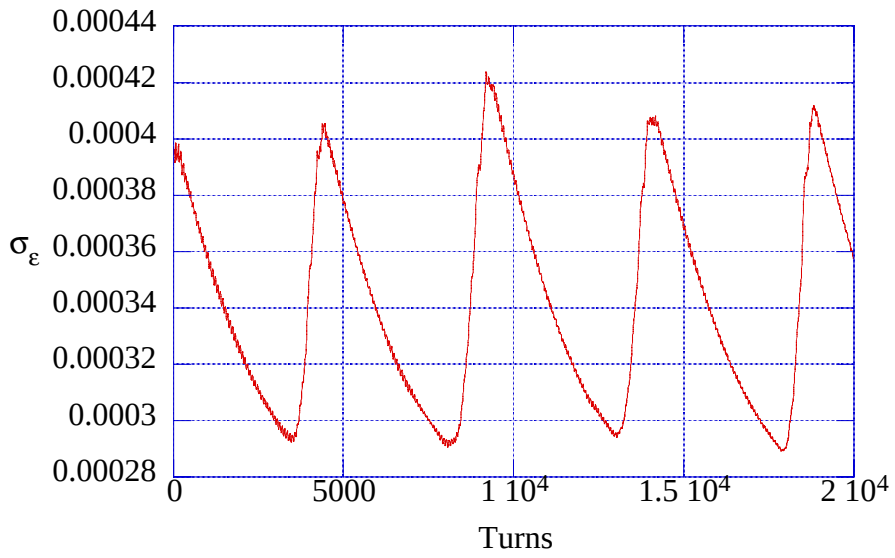

Figure 2: Energy spread vs number of turns for a pure inductive impedance obtained with a simulation code.

produced by the beam (wakefields) interact with the beam itself as in a loop system. To introduce wake fields, we consider the coordinate system of Figure 3 and call $q_1\left(z_1, \mathbf{r_1}\right)$ a charge traveling with constant velocity $v = c$ along a trajectory parallel to the axis of the vacuum chamber. The longitudinal Lorentz force generated by q_1 acting on a test charge $q\left(z, \mathbf{r}\right)$ following q_1 at a distance $\Delta z = z_1 - z$ produces on this charge an energy variation given by

$$U_{||}\left(\mathbf{r}, \mathbf{r}_1; \Delta z\right) = -\int_{\text{Str}} F_{||}\left(z, \mathbf{r}, z_1, \mathbf{r}_1; t\right) dz \qquad t = \left(z_1 + \Delta z\right)/c. \tag{1}$$

The quantity $U_{||}$ represents the energy lost (> 0) or gained (< 0) by a charge passing through a machine device, due to electromagnetic forces parallel to the particle motion. We assume that the relative energy change is so small that it does not produce any appreciable variation of the relativistic factor β.

We define the longitudinal wake function as the energy variation of a test charge q per unit charge q and q_1

$$w_{||}\left(\mathbf{r}, \mathbf{r}_1; \Delta z\right) = \frac{U_{||}\left(\mathbf{r}, \mathbf{r}_1; \Delta z\right)}{q q_1}. \tag{2}$$

It can be thought of as the Green function that describes the longitudinal response of the structure to an impulsive source. It depends only on the geometrical and electro-

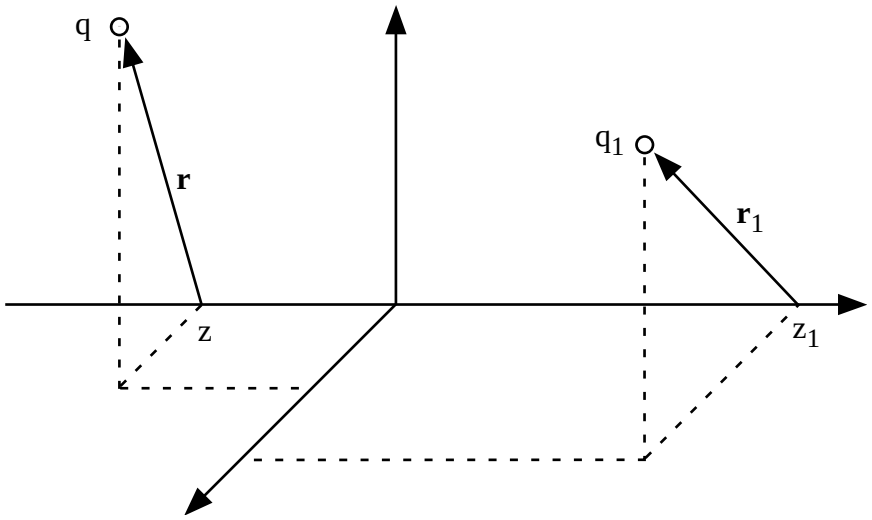

Figure 3: System of reference coordinate.

magnetic properties of the device. For $\beta = 1$, according to the causality principle, the wake function is zero for $\Delta z < 0$, i. e. for a test charge ahead of the leading one.

In general, the beam pipe is composed of structures having symmetric shapes. In the case of cylindrical symmetry it is convenient to expand the wake function in multi-polar terms. For the longitudinal case, around the vacuum chamber axis, the first monopole term is dominant and the longitudinal wakefield becomes a function only of Δz.

For a longitudinal bunch distribution $\rho(z)$ that satisfies the normalization condition

$$\int_{-\infty}^{\infty} \rho(z)\, dz = 1 \tag{3}$$

the energy variation of a test charge at position z inside the bunch is

$$U_{||}(z) = e^2 N_p \int_{-\infty}^{\infty} \rho(z')\, w_{||}(z' - z)\, dz' \tag{4}$$

where N_p is the total number of particles in the bunch. We often call the bunch- wake-potential the energy lost $U_{||}(z)$ normalized to $e^2 N_p$.

2.2 Coupling Impedance

We define the longitudinal coupling impedance[2] as the Fourier transform of the wake function

$$Z_{||}(\mathbf{r}, \mathbf{r}_1; \omega) = \frac{1}{c} \int_{-\infty}^{\infty} w_{||}(\mathbf{r}, \mathbf{r}_1; \Delta z) \exp\left[-i\omega \frac{\Delta z}{c}\right] d(\Delta z)\,. \tag{5}$$

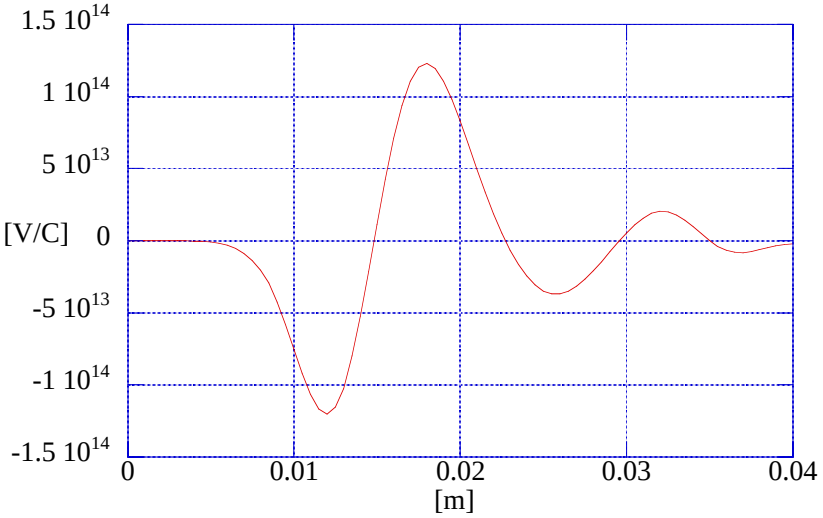

Figure 4: DAΦNE wake potential.

A real accelerator is composed of many devices connected by a vacuum chamber. For such a complicated structure, it is impossible to obtain analytical solutions of Maxwell's equations. Usually, numerical codes for the finite differences, which solve Maxwell's equations in the time domain, are used. Because of the CPU time limitations, we can analyze only a single device, or a few of them connected to an infinite pipe. Then the contributions of all the pieces are summed up to get the whole wake function. It is worth noting that this procedure might fail at high frequencies where the fields propagate in the vacuum chamber from one device to another, producing interference effects. Furthermore, numerical codes allow us to obtain only the wake potential of a distribution rather then the impulsive wake function. In Figure 4 we show as an example the wake potential of the DAΦNE machine[3] at INFN - LNF for a 2.5-mm Gaussian bunch obtained with the codes MAFIA[4] and ABCI[5].

For the study of collective effects it is convenient to distinguish between single-bunch dynamics, where the particles experience the wakefields produced by the other particles of the same bunch, and multibunch or multiturn dynamics, where the electromagnetic fields trapped in resonant structures influence other bunches or the same bunch in successive passages. Such a distinction applies also to the wakefields, called respectively short-range and long-range wakefields.

2.3 Short-Range Wakefields

Electromagnetic fields that vanish after a distance of a few bunch lengths are usually called short-range wakefields. With short-range wakefields we have a low frequency resolution of the Fourier transform, and therefore of the impedance. Even though impedance is a complicated function of frequency, with many sharp peaks, in the study of single-bunch dynamics influenced by short-range wakefields, the bunch can not resolve the details of the sharp resonances, and it rather experiences an average effect. The corresponding impedance is then smoother and broader than the actual machine impedance, and is called broad-band impedance.

For an approach to single-bunch collective effects, we can obtain the machine broad-band impedance with numerical codes. Usually the frequency behavior is simplified by using some impedance models. Such models, characterized by a small number of parameters, are useful also in the design study of the machine, when not all the devices are defined and known.

The first model historically introduced in the study of single-bunch longitudinal dynamics[6] is the so-called broad-band resonator:

$$Z_{||}(\omega) = \frac{R_s}{1 + iQ\left(\dfrac{\omega}{\omega_r} - \dfrac{\omega_r}{\omega}\right)}. \tag{6}$$

Only three parameters are needed to determine its frequency behavior: the shunt resistance R_s, the quality factor Q, and the resonant frequency ω_r. Usually $Q \simeq 1$, ω_r is the frequency cut-off of the beam pipe, and R_s accounts for the parasitic energy loss.

The corresponding longitudinal wake function is given by the inverse Fourier transform of Eq. (5), with $Z_{||}(\omega)$ expressed by Eq. (6):

$$w_{||}(\Delta z) = \frac{\omega_r R_s}{Q} \exp\left(-\frac{\Gamma \Delta z}{c}\right)\left[\cos\left(\frac{\omega_n \Delta z}{c}\right) - \frac{\omega_r}{2Q\omega_n}\sin\left(\frac{\omega_n \Delta z}{c}\right)\right] H(\Delta z) \tag{7}$$

where

$$\Gamma = \frac{\omega_r}{2Q} \qquad \omega_n^2 = \omega_r^2 - \Gamma^2 \tag{8}$$

and $H(\Delta z)$ is the step function.

It is worth noting that because of the low value of the quality factor, the short-range wake function vanishes rapidly with Δz.

Other impedance models have been proposed[7]. Among them we present one based on a phenomenological approach[8], which describes the impedance as an expansion in terms of $\sqrt{\omega}$ of the kind

$$Z_{||}(\omega) = i\omega L + R + [1 + i\,\mathrm{sgn}(\omega)]\sqrt{|\omega|}B + \frac{1 - i\,\mathrm{sgn}(\omega)}{\sqrt{|\omega|}}Z_c + \ldots. \tag{9}$$

Every term of the expansion has a clear physical interpretation. The first term represents the inductive impedance at low frequencies typical of small discontinuities. Often it is the main contribution to the total impedance, producing a symmetric distortion of the bunch. The second term is due mainly to the RF cavities or resonant devices, and produces a shift of the bunch center of mass and a distortion of its shape. The third term represents the resistive wall impedance due to the finite conductivity of the beam pipe material, and the fourth has the same dependence on ω as the impedance of a cavity with attached tubes at high frequencies. For long enough bunches the first two terms of Eq. (9) give the main contribution to the total broad-band impedance, and are sufficient to describe the single-bunch behavior. Moreover we can obtain the values of the two parameters R and L from measurements of bunch length and synchronous phase shift versus current. The longitudinal wake function corresponding to this model with just R and L is given by

$$w_{||}\left(\Delta z\right) = c^2 L \delta'\left(\Delta z\right) + cR\delta\left(\Delta z\right) \tag{10}$$

where δ and δ' are respectively the symbolic Dirac delta function and its derivative. Such a wake function can be easily handled analytically.

3 Equations of Motion

3.1 Single-Particle Motion

The single-particle equations of motion are

$$\dot{z} = \frac{\Delta z}{T_0} = \frac{z\left(t\right) - z\left(t - T_0\right)}{T_0} = -c\alpha_c \varepsilon, \tag{11}$$

$$\dot{\varepsilon} = \frac{\Delta \varepsilon}{T_0} = \frac{\varepsilon\left(t\right) - \varepsilon\left(t - T_0\right)}{T_0} = \frac{eV\left(z\right) - U_0}{T_0 E_0} - \frac{D}{T_0}\varepsilon - \frac{R\left(T_0\right)}{T_0 E_0} \tag{12}$$

where z is the longitudinal displacement of a particle with respect to the synchronous one ($z > 0$ means particle ahead), T_0 the revolution period, c the speed of light, α_c the momentum compaction, ε the energy variation with respect to the nominal energy E_0, $V(z)$ the voltage seen by the particle in one turn, and U_0 the energy lost per turn. A particle radiates an energy per turn equal to $U_0 + D\varepsilon + R\left(T_0\right)$ where $R\left(T_0\right)$ is a stochastic variable that accounts for the quantum fluctuations. The damping coefficient D is equal to $2T_0$ divided by the damping time τ_ε.

Since $V\left(z\right)$ is the contribution of the RF cavities and of the longitudinal wake fields, we can write Eq. (12) as

$$\dot{\varepsilon} = \frac{eV_{RF}\left(z\right) - U_0}{T_0 E_0} - \frac{e^2 N_p}{T_0 E_0}\int_{-\infty}^{\infty} \rho\left(z'\right) w_{||}\left(z' - z\right) dz' - \frac{D}{T_0}\varepsilon - \frac{R\left(T_0\right)}{T_0 E_0}. \tag{13}$$

Equations (11) and (13) describe the longitudinal dynamics of a single particle in a circular accelerator. The potential well in which the particle motion is confined is given by

$$\varphi(z) = \frac{\alpha_c}{L_0}\int_0^z \left[eV_{RF}(z') - U_0\right] dz' - \frac{\alpha_c e^2 N_p}{L_0}\int_0^z dz' \int_{-\infty}^{\infty} \rho(z'')\, w_{||}(z''-z')\, dz''. \quad (14)$$

For such a motion the Hamiltonian, defined as

$$H(z,\varepsilon) = \frac{1}{2}c\alpha_c\varepsilon^2 + \frac{c}{\alpha_c E_0}\varphi(z), \quad (15)$$

satisfies the relations

$$\begin{aligned} \frac{\partial H}{\partial \varepsilon} &= -\dot{z}, \\ \frac{\partial H}{\partial z} &= \dot{\varepsilon} + \frac{D}{T_0}\varepsilon + \frac{R(T_0)}{T_0 E_0} \end{aligned} \quad (16)$$

where the last two terms in the second relation represent the non-conservative components of the system.

Since the revolution period T_0 is much smaller than the synchrotron period, we can make a linear expansion of $z(t)$ and $\varepsilon(t)$:

$$\begin{aligned} z(t) &= z(t-T_0) + \dot{z}T_0, \\ \varepsilon(t) &= \varepsilon(t-T_0) + \dot{\varepsilon}T_0, \end{aligned} \quad (17)$$

and

$$\begin{aligned} [z+dz]_t &= [z+dz]_{t-T_0} + \dot{z}|_{z+dz,\varepsilon}\, T_0, \\ [\varepsilon+d\varepsilon]_t &= [\varepsilon+d\varepsilon]_{t-T_0} + \dot{\varepsilon}|_{z,\varepsilon+d\varepsilon}\, T_0. \end{aligned} \quad (18)$$

By using now the relations (16) for $\dot{z}$ and $\dot{\varepsilon}$, and by noting that the partial derivative of the Hamiltonian with respect to z or ε is a function of z or ε only, we have

$$\begin{aligned} \dot{z}|_{z+dz,\varepsilon} &= -\frac{\partial H}{\partial \varepsilon}, \\ \dot{\varepsilon}|_{z,\varepsilon+d\varepsilon} &= \frac{\partial H}{\partial z} - \frac{D}{T_0}\varepsilon - \frac{D}{T_0}d\varepsilon - \frac{R(T_0)}{T_0 E_0}. \end{aligned} \quad (19)$$

If we subtract Eq. (17) from Eq. (18), using the above relation and Eq. (16), we obtain

$$\begin{aligned} dz|_t &= dz|_{t-T_0}, \\ d\varepsilon|_t &= d\varepsilon|_{t-T_0}(1-D), \end{aligned} \quad (20)$$

which give the relation between an infinitesimal area in the phase space at time t and the corresponding one at time $t - T_0$.

Before continuing our analysis, we examine the quantity $R(T_0)$. It represents the difference between the actual energy lost per turn by a particle and its average value. It is a stochastic variable describing the quantum fluctuations, and its average value is zero. We define the probability density $P[R(T_0)]$ such that $P[R'(T_0)]\,dR'(T_0)$ represents the probability that a particle, during a revolution period, radiates an energy equal to $U_0 + D\varepsilon + R(T_0)$ with $R(T_0)$ between $R'(T_0)$ and $R'(T_0) + dR'(T_0)$.

3.2 Transport and Fokker-Planck Equations

In order to study the collective single-bunch effects, we need to move from the single-particle equation of motion to an equation for an ensemble of particles. To this end we consider the longitudinal single-bunch distribution function $\Psi(z, \varepsilon; t)$ defined such that $\Psi(z, \varepsilon; t)\,dzd\varepsilon$ represents the probability of finding at time t a particle in the area $(z, z + dz, \varepsilon, \varepsilon + d\varepsilon)$ of the phase space. It satisfies the normalization condition

$$\int_{-\infty}^{\infty}\int_{-\infty}^{\infty}\Psi(z, \varepsilon; t)\,dzd\varepsilon = 1. \tag{21}$$

Its projection on the z axis gives the longitudinal bunch distribution $\rho(z)$ introduced in Eq. (4),

$$\rho(z; t) = \int_{-\infty}^{\infty}\Psi(z, \varepsilon; t)\,d\varepsilon. \tag{22}$$

We aim to derive a differential equation that describes the time evolution of the longitudinal distribution function[9].

The probability that a particle at time t has its representative point of the phase space in the area $dzd\varepsilon$ with center (z, ε) is, by definition, $\Psi(z, \varepsilon; t)\,dzd\varepsilon|_t$. The same quantity is also equal to the probability that the particle at time $t - T_0$ was in any point of the phase space such that

$$\begin{aligned} z(t - T_0) &= z(t) - \dot{z}T_0 = z(t) + \frac{\partial H}{\partial \varepsilon}T_0, \\ \varepsilon(t - T_0) &= \varepsilon(t) - \dot{\varepsilon}T_0 = \varepsilon(t) - \frac{\partial H}{\partial z}T_0 + D\varepsilon + \frac{R(T_0)}{E_0}, \end{aligned} \tag{23}$$

and, in a revolution period, it radiated an energy equal to $U_0 + D\varepsilon + R(T_0)$. Since the probability of radiating such an energy is $P[R(T_0)]\,dR(T_0)$, we can write

$$\begin{aligned} &\Psi[z(t), \varepsilon(t); t]\,dzd\varepsilon|_t \\ &\qquad = \int_{-\infty}^{\infty}\Psi[z(t - T_0), \varepsilon(t - T_0); t - T_0]\,dzd\varepsilon|_{t-T_0}\,P[R(T_0)]\,dR(T_0) \end{aligned} \tag{24}$$

where $R(T_0)$ is a stochastic variable that can assume any value from $-\infty$ to $+\infty$ with a given probability $P[R(T_0)]$.

The integral equation (24) is known as the transport equation, and it allows us to follow the time evolution of the distribution function $\Psi(z, \varepsilon; t)$ once the Hamiltonian and the probability function $P[R(T_0)]$ are known.

From the transport equation we can derive a differential equation by using the Fokker-Planck method[10]. This consists of expanding Eq. (24) in time around t keeping only linear terms. As shown in Appendix A, we obtain

$$\frac{\partial \Psi}{\partial t} = \frac{\partial \Psi}{\partial z}\frac{\partial H}{\partial \varepsilon} - \frac{\partial \Psi}{\partial \varepsilon}\frac{\partial H}{\partial z} + \frac{D}{T_0}\left(\Psi + \varepsilon\frac{\partial \Psi}{\partial \varepsilon}\right) + \frac{1}{2}\frac{\partial^2 \Psi}{\partial \varepsilon^2}\frac{\overline{R^2(T_0)}}{T_0 E_0^2} \tag{25}$$

where $\overline{R^2(T_0)}$ is the variance of the radiated energy defined as

$$\overline{R^2(T_0)} = \int_{-\infty}^{\infty} R^2(T_0)\, P[R(T_0)]\, dR(T_0). \tag{26}$$

In Eq. (25), known as the Fokker-Planck equation or diffusion equation, the first two terms in the right side represent the conservative part of the system, and the other two are related to the radiation process: damping and quantum fluctuations respectively. These effects produce an equilibrium energy distribution with an RMS, known also as the natural energy spread, equal to

$$\sigma_{\varepsilon 0} = \sqrt{\frac{\overline{R^2(T_0)}}{2DE_0^2}}. \tag{27}$$

All the fundamental elements that characterize single-bunch and multibunch collective phenomena are included in the equation. Unfortunately, there is no general solution for it; however, it gives useful information about collective effects.

4 Bunch Distortion below Threshold

4.1 Stationary Solution

As a first application of the Fokker-Planck equation, we look for its stationary solution, that is, a distribution function independent of time, for which

$$\frac{\partial \Psi}{\partial t} = 0 \qquad \Rightarrow \qquad \Psi(z, \varepsilon; t) = \Psi_0(z, \varepsilon). \tag{28}$$

With such a condition it is possible to find a general solution of the Fokker-Planck equation of the kind

$$\Psi_0(z, \varepsilon) = \overline{\Psi} \exp\left[-\frac{H_0(z, \varepsilon)}{\overline{H}}\right] \tag{29}$$

where the subscript zero to Ψ and H means time independent, the constant $\overline{\Psi}$ is given by the normalization condition Eq. (21), and the constant $\overline{H}$ is

$$\overline{H} = \frac{c\alpha_c \overline{R^2\left(T_0\right)}}{2DE_0^2}. \tag{30}$$

Equation (29) is known as the Haissinski equation[11], and it gives the equilibrium distribution of a bunch in the presence of self-induced wakefields and external RF voltage.

A first important observation is that the distribution function can be factorized, and the energy distribution is independent of the wakefields and of the potential well where the particles are confined. In fact, if we write explicitly the Hamiltonian of Eq. (29), and use Eq. (30), we get

$$\Psi_0\left(z,\varepsilon\right) = \overline{\Psi}\exp\left[-\frac{DE_0^2\varepsilon^2}{\overline{R^2\left(T_0\right)}} - \frac{c}{\alpha_c E_0 \overline{H}}\varphi\left(z\right)\right], \tag{31}$$

from which it is easy to see that the term related to the energy always gives a Gaussian distribution with an RMS that comes out of the balance between the damping coefficient and the quantum fluctuation noise only [see Eq. (27)].

For the longitudinal distribution function, if we integrate Eq. (31) in ε, and write explicitly the potential as given by Eq. (14), we get

$$\rho_0\left(z\right) = \overline{\rho}\exp\left[-\frac{1}{L_0 E_0 \alpha_c \sigma_{\varepsilon 0}^2}\int_0^z \left[eV_{RF}\left(z'\right) - U_0\right]dz' + \right.$$
$$\left. \frac{e^2 N_p}{L_0 E_0 \alpha_c \sigma_{\varepsilon 0}^2}\int_0^z dz' \int_{-\infty}^{\infty} \rho_0\left(z''\right) w_{||}\left(z''-z'\right)dz''\right]. \tag{32}$$

The above equation, which is sometimes referred to as the Haissinski equation instead of Eq. (29), is an integral equation in the function $\rho\left(z\right)$.

4.2 Natural Regime

Let us consider first the case without wakefields, i. e. the natural regime. The longitudinal bunch distribution is given only by the RF voltage:

$$V_{RF}\left(z\right) = \hat{V}\cos\left(\phi_s - 2\pi h\frac{z}{L_0}\right) \tag{33}$$

where the synchronous phase $\phi_s = \omega_{RF} t_s$ is given by the condition

$$\cos\left(\phi_s\right) = \frac{U_0}{e\hat{V}}. \tag{34}$$

In the usual case $2\pi hz \ll L_0$, we can linearly expand $V_{RF}(z)$ around $z = 0$, obtaining

$$V_{RF}(z) = \hat{V}\cos(\phi_s) + \frac{2\pi h\hat{V}\sin(\phi_s)}{L_0}z. \tag{35}$$

If we insert Eq. (35) into Eq. (32) and use Eq. (34), we obtain

$$\rho_0(z) = \overline{\rho}\exp\left[-\frac{\omega_{s0}^2 z^2}{2\alpha_c^2 c^2\sigma_{\varepsilon 0}^2}\right] = \overline{\rho}\exp\left[-\frac{z^2}{2\sigma_{z0}^2}\right] \tag{36}$$

where we have used the natural angular synchrotron frequency

$$\omega_{s0}^2 = \frac{c^2\alpha_c 2\pi he\hat{V}\sin(\phi_s)}{L_0^2 E_0}. \tag{37}$$

The longitudinal bunch distribution is then a Gaussian distribution with an RMS given by

$$\sigma_{z0} = \frac{\alpha_c c\sigma_{\varepsilon 0}}{\omega_{s0}} \tag{38}$$

and with a constant $\overline{\rho}$ obtained by the normalization condition Eq. (3),

$$\overline{\rho} = \frac{1}{\sqrt{2\pi}\sigma_{z0}}. \tag{39}$$

4.3 Wakefield Effects

4.3.1 Resistive Impedance

If we include the effects of the wakefield, we find that the bunch distribution is distorted. This effect can be studied analytically in the case of a pure resistive impedance for which, assuming the linear expansion of the RF voltage, Eq. (32) becomes

$$\rho_0(z) = \overline{\rho}\exp\left[-\frac{z^2}{2\sigma_{z0}^2} + \frac{e^2 N_p cR}{L_0 E_0\alpha_c\sigma_{\varepsilon_0}^2}\int_0^z \rho_0(z')\,dz'\right]. \tag{40}$$

As shown in Appendix B, the analytical solution of the above equation is

$$\rho_0(z) = \frac{\exp\left(-\dfrac{z^2}{2\sigma_{z0}^2}\right)}{\xi_1\sigma_{z0}\sqrt{\dfrac{\pi}{2}}\left[\coth\left(\dfrac{\xi_1}{2}\right) - \operatorname{erf}\left(\dfrac{z}{\sqrt{2}\sigma_{z0}}\right)\right]} \tag{41}$$

where the error function is

$$\operatorname{erf}(x) = \frac{2}{\sqrt{\pi}}\int_0^z \exp\left(-x^2\right)dx \tag{42}$$

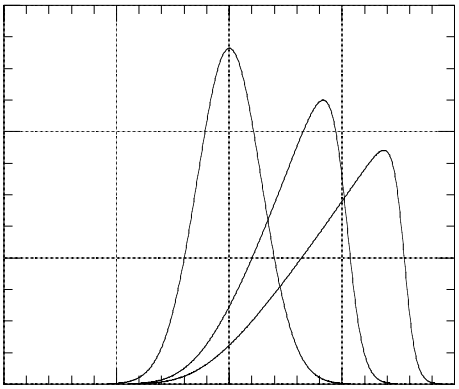

Figure 5: Bunch shapes at different N_p for pure resistive impedance.

and

$$\xi_1 = \frac{e^2 N_p c R}{L_0 E_0 \alpha_c \sigma_{\varepsilon 0}^2}. \tag{43}$$

A pure resistive impedance distorts the bunch and shifts its center of mass ahead, but does not change its RMS much. In Figure 5 we show an example of longitudinal bunch distribution at different N_p.

4.3.2 Inductive Impedance

In the case of pure inductive impedance, the bunch distribution is given by

$$\rho_0(z) = \overline{\rho} \exp\left[-\frac{z^2}{2\sigma_{z0}^2} - \frac{e^2 N_p c^2 L}{L_0 E_0 \alpha_c \sigma_{\varepsilon 0}^2} \rho_0(z)\right] \tag{44}$$

which can be solved with numerical tools. From Figure 6, we see that the inductive impedance does not influence the position of the bunch center of mass, but increases only the bunch length. The distribution function is no longer Gaussian, but tends to become parabolic, especially around the bunch center.

4.3.3 Broad-Band Resonator Impedance

With the broad-band resonator model, as well as with any general wake function, it is convenient to transform Eq. (32) by introducing the wake potential of a unitary step distribution

$$S(z) = \int_0^z w_{||}(z')\, dz' \tag{45}$$

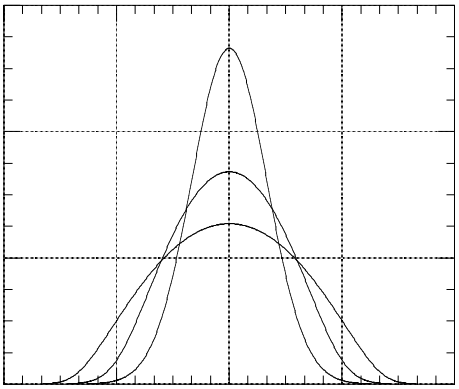

Figure 6: Bunch shapes at different N_p for pure inductive impedance.

with which we can express Eq. (32) as

$$\rho_0\left(z\right) = \overline{\rho_1}\exp\left[-\frac{z^2}{2\sigma_{z0}^2} - \frac{e^2 N_p}{L_0 E_0 \alpha_c \sigma_{\varepsilon 0}^2}\int_{-\infty}^{\infty}\rho_0\left(z'+z\right)S\left(z'\right)dz'\right]. \tag{46}$$

The solution of the above equation for the resonator impedance is given in Figure 7 for different values of N_p.

5 Threshold Hunting

5.1 Perturbation Theory

Comparing the stationary distribution with the experimental observations in a real machine, we find that they agree only at low current, where the energy spread is constant, and the longitudinal bunch distribution is distorted according to the potential well theory. However, when N_p is high, we can no longer explain the experimental observations in terms of a stationary solution. We need to explore a new dynamical regime, where the distribution function is a function of time.

In this section, we show a perturbation method generally used to obtain the behavior of $\Psi\left(z,\varepsilon;t\right)$ around the stationary solution $\Psi_0\left(z,\varepsilon\right)$[12,13].

We start by linearizing $\Psi\left(z,\varepsilon;t\right)$:

$$\Psi\left(z,\varepsilon;t\right) = \Psi_0\left(z,\varepsilon\right) + \Psi_1\left(z,\varepsilon;t\right) \tag{47}$$

where $\Psi_1\left(z,\varepsilon;t\right)$ is a perturbation of $\Psi_0\left(z,\varepsilon\right)$. Similar expansions apply also to the single-particle potential

$$\varphi\left(z\right) = \varphi_0\left(z\right) + \varphi_1\left(z;t\right) \tag{48}$$

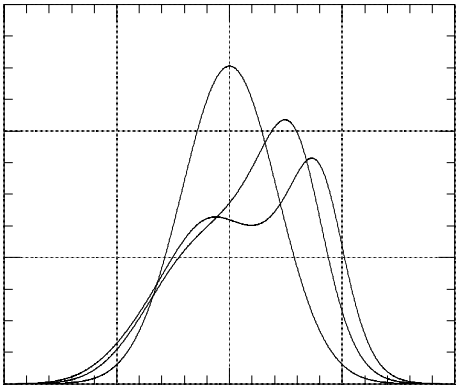

Figure 7: Bunch shapes at different N_p for the broad band resonator.

and to the Hamiltonian

$$H\left(z,\varepsilon;t\right)=H_0\left(z,\varepsilon\right)+H_1\left(z;t\right) \tag{49}$$

where

$$H_1\left(z;t\right)=\frac{c}{\alpha_c E_0}\varphi_1\left(z;t\right)=-\frac{ce^2N_p}{E_0L_0}\int_0^z dz'\int_{-\infty}^{\infty}\rho_1\left(z'';t\right)w_{||}\left(z''-z'\right)dz'' \tag{50}$$

and

$$\rho_1\left(z;t\right)=\int_{-\infty}^{\infty}\Psi_1\left(z,\varepsilon;t\right)d\varepsilon. \tag{51}$$

If we substitute Eqs. (47) and (49) into the Fokker-Planck equation, and observe that $\Psi_0\left(z,\varepsilon\right)$ satisfies the stationary equation, we get

$$\frac{\partial\Psi_1}{\partial t}=\frac{\partial\Psi_1}{\partial z}\frac{\partial H_0}{\partial\varepsilon}-\frac{\partial\Psi_0}{\partial\varepsilon}\frac{\partial H_1}{\partial z}-\frac{\partial\Psi_1}{\partial\varepsilon}\frac{\partial H_0}{\partial z}-\frac{\partial\Psi_1}{\partial\varepsilon}\frac{\partial H_1}{\partial z}+\frac{D}{T_0}\left(\Psi_1+\varepsilon\frac{\partial\Psi_1}{\partial\varepsilon}\right)+\frac{1}{2}\frac{\partial^2\Psi_1}{\partial\varepsilon^2}\frac{\overline{R^2\left(T_0\right)}}{T_0E_0^2}. \tag{52}$$

We now ignore the second-order terms and the effects of radiation damping and fluctuation noise on the perturbation function Ψ_1. By introducing the two action-angle variables, J and ϕ, as shown in Appendix C, we get

$$\frac{\partial\Psi_1}{\partial t}=-\omega_s\left(J\right)\frac{\partial\Psi_1}{\partial\phi}+\frac{c^2\alpha_ce^2N_p}{E_0L_0\omega_s\left(J\right)}\frac{\partial\Psi_0}{\partial J}\varepsilon\int_{-\infty}^{\infty}\rho_1\left(z';t\right)w_{||}\left(z'-z\right)dz'. \tag{53}$$

In order to find the solution of Eq. (53), we note that $\Psi_1\left(J,\phi;t\right)$ is periodic in ϕ, and it can then be expanded as a Fourier series, while for the time dependence, we apply

the modal analysis in the frequency domain, which allows us to write

$$\Psi_1(J,\phi;t) = \exp[i\Omega t]\sum_{m=-\infty}^{\infty} R_m(J)\exp[-im\phi] \tag{54}$$

which, introduced into Eq. (53), gives

$$i\Omega\sum_{m=-\infty}^{\infty} R_m(J)\exp[-im\phi] = i\omega_s(J)\sum_{n=-\infty}^{\infty} nR_n(J)\exp[-in\phi] + \frac{c^2\alpha_c e^2 N_p}{E_0 L_0\omega_s(J)}\frac{\partial\Psi_0}{\partial J}\varepsilon\sum_{l=-\infty}^{\infty}\int_0^{2\pi} d\phi'\int_0^{\infty} R_l(J')\exp[-il\phi']\, w_{||}(z'-z)\, dJ'. \tag{55}$$

Since the value of m in Eq. (54) specifies the angular dependence of the mth term of the Fourier expansion, m is also called the azimuthal number, and the corresponding $R_m(J)$ is called the radial function. We now exploit the symmetry of $w_{||}(z'-z)$ with respect to the angle variable ϕ' and the fact that $\varepsilon(J,\phi)$ is antisymmetric in ϕ. Multiplying by $\exp[im'\phi]$ and integrating in ϕ from 0 to 2π, we obtain

$$[\Omega - m\omega_s(J)]\, R_m(J) = \frac{c^2\alpha_c e^2 N_p}{2\pi E_0 L_0\omega_s(J)}\frac{\partial\Psi_0}{\partial J}\sum_{l=-\infty}^{\infty}\int_0^{2\pi} d\phi \times\int_0^{2\pi} d\phi'\int_0^{\infty}\varepsilon(J,\phi)\, R_l(J')\sin(m\phi)\cos(l\phi')\, w_{||}(z'-z)\, dJ'. \tag{56}$$

In terms of the coupling impedance this becomes

$$[\Omega - m\omega_s(J)]\, R_m(J) = \frac{c^2\alpha_c e^2 N_p}{4\pi^2 E_0 L_0\omega_s(J)}\frac{\partial\Psi_0}{\partial J}\sum_{l=-\infty}^{\infty}\int_0^{2\pi} d\phi\int_0^{2\pi} d\phi' \times\int_{-\infty}^{\infty} d\omega\int_0^{\infty}\varepsilon(J,\phi)\, R_l(J')\sin(m\phi)\cos(l\phi')\exp\left[i\frac{\omega}{c}(z'-z)\right] Z_{||}(\omega)\, dJ'. \tag{57}$$

Equations (56) and (57) represent a generic term of the infinite set of integral homogeneous equations for $R_m(J)$. If we treat the whole set of equations as an eigenvalue problem in Ω, we get that the number of eigenvalues is the same as those of m, i. e. infinite. Each $\Omega^{(m)}$ is called a coherent frequency of the azimuthal oscillation mode m. In the limit of $N_p \to 0$, we easily obtain

$$\begin{aligned}\omega_s(J) &\to \omega_{s0},\\ \Omega^{(m)} &= m\omega_{s0}.\end{aligned} \tag{58}$$

In the next sections we show two methods used to solve Eq. (57).

5.2 Sacherer Equation

An attempt to evaluate the threshold of microwave instability through mode coupling is based on the simplifying hypothesis that single-particle motion is governed by a quadratic form of the Hamiltonian, of the kind

$$H\left(z,\varepsilon\right)=\frac{1}{2}c\alpha_c\varepsilon^2+\frac{1}{2}\frac{\omega_s^2}{c\alpha_c}z^2, \tag{59}$$

which corresponds to a linear RF voltage. The hypotheses behind Eq. (59) are Ψ_0 stationary and symmetric and ω_s independent of the amplitude J.

The equations of motion of a single particle, ignoring the effects of radiation damping and quantum fluctuations, can be expressed as

$$\begin{aligned} z&=\sqrt{\frac{2c\alpha_c J}{\omega_s}}\cos\left[\phi\left(t\right)\right],\\ \varepsilon&=\sqrt{\frac{2\omega_s J}{c\alpha_c}}\sin\left[\phi\left(t\right)\right]. \end{aligned} \tag{60}$$

If we substitute Eqs. (60) into Eq. (57) and use the relations

$$\int_0^{2\pi}\sin\left(\phi\right)\sin\left(m\phi\right)\exp\left[-ia\cos\left(\phi\right)\right]d\phi=i2\pi i^{-m}\frac{m}{a}J_m\left(a\right) \tag{61}$$

and

$$\int_0^{2\pi}\cos\left(l\phi\right)\exp\left[ia\cos\left(\phi\right)\right]d\phi=2\pi i^l J_l\left(a\right) \tag{62}$$

where $J_m\left(x\right)$ is a Bessel function of first kind and mth order, we get

$$\begin{aligned} \left[\Omega-m\omega_s\right]R_m\left(J\right)=i\frac{mc^2e^2N_p}{E_0L_0}\frac{\partial\Psi_0}{\partial J}\sum_{l=-\infty}^{\infty}i^{l-m}\\ \times\int_{-\infty}^{\infty}\frac{Z_{||}\left(\omega\right)}{\omega}J_m\left(\omega\sqrt{\frac{2\alpha_c J}{c\omega_s}}\right)d\omega\int_0^{\infty}R_l\left(J'\right)J_l\left(\omega\sqrt{\frac{2\alpha_c J'}{c\omega_s}}\right)dJ' \end{aligned} \tag{63}$$

where we have considered $\omega\left(J\right)=\omega_s$. In order to express the eigenvalue problem in a simple form, we introduce the two functions

$$G_{ml}\left(J,J'\right)=i\frac{mc^2e^2N_p\overline{\Psi}}{\omega_sE_0L_0}\int_{-\infty}^{\infty}\frac{Z_{||}\left(\omega\right)}{\omega}J_m\left(\omega\sqrt{\frac{2\alpha_c J}{c\omega_s}}\right)J_l\left(\omega\sqrt{\frac{2\alpha_c J'}{c\omega_s}}\right)d\omega \tag{64}$$

and

$$w\left(J\right)=-\frac{1}{\overline{\Psi}}\frac{\partial\Psi_0}{\partial J} \tag{65}$$

with $\overline{\Psi}$ already defined in Eq. (29), and write Eq. (63) as

$$\left[\frac{\Omega}{\omega_s} - m\right] R_m(J) = -w(J) \sum_{l=-\infty}^{\infty} i^{l-m} \int_0^{\infty} G_{ml}(J, J') R_l(J') \, dJ', \tag{66}$$

known as the Sacherer integral equation for longitudinal instabilities.

5.3 A Method of Solving the Sacherer Equation

Different methods have been proposed for solving Eq. (66) [14]. Here we show the one that uses the expansion of the radial function $R_m(J)$ in orthogonal polynomials:

$$R_m(J) = w(J) \sum_{k=0}^{\infty} a_{mk} f_{|m|k}(J). \tag{67}$$

The absolute value of m in the polynomials $f_{|m|k}(J)$ is due to the property that the radial distributions of the terms $\pm m$ are equal. The functions $f_{|m|k}(J)$ satisfy the normalization condition

$$\int_0^{\infty} w(J) f_{|m|k}(J) f_{|m|l}(J) \, dJ = \delta_{kl} \tag{68}$$

where $w(J)$ is a weight function and δ_{kl} is the Kronecher symbol.

Introducing Eq. (67) into Eq. (66), multiplying by $f_{|m|p}(J)$, and integrating in J from 0 to ∞, we obtain

$$\left[\frac{\Omega}{\omega_s} - m\right] a_{mp} = \sum_{l=-\infty}^{\infty} \sum_{k=0}^{\infty} M_{pk}^{ml} a_{lk} \tag{69}$$

with

$$M_{pk}^{ml} = -i^{l-m} \int_0^{\infty} w(J) f_{|m|p}(J) \, dJ \int_0^{\infty} G_{ml}(J, J') w(J') f_{|l|k}(J') \, dJ'. \tag{70}$$

Equation (69) is the generic term of a homogeneous system of equations, with m ranging from $-\infty$ to ∞ and p from 0 to ∞. If we consider the system as an eigenvalue problem, a_{mp} being the eigenvectors, the eigenvalues $\Omega^{(m,p)}$ can be evaluated once the orthogonal polynomials $f_{|m|p}(J)$ are known. These last depend only on the weight function $w(J)$, which, in turn, depends on the stationary distribution function $\Psi_0(J)$.

For the Gaussian distribution function given by Eq. (29), as shown in Appendix D, we get

$$M_{pk}^{ml} = -i \frac{c^2 e^2 N_p}{2\pi \omega_s E_0 L_0 \sigma_z \sigma_{\varepsilon 0}} i^{|l|-|m|} \frac{m}{\sqrt{p!\,(|m|+p)!\,k!\,(|l|+k)!}} \times \int_{-\infty}^{\infty} \frac{Z_{||}(\omega)}{\omega} \left(\frac{\omega \sigma_z}{\sqrt{2}c}\right)^{|m|+|l|+2p+2k} \exp\left[-\frac{\omega^2 \sigma_z^2}{c^2}\right] d\omega. \tag{71}$$

For the RL impedance, the integral in ω can be solved, giving

$$M_{pk}^{ml} = -i\frac{c^2e^2N_p}{2\pi\omega_s E_0 L_0 \sigma_z \sigma_{\varepsilon 0}} \frac{i^{|l|-|m|} m 2^{-\left(\frac{|m|+|l|}{2}+p+k\right)}}{\sqrt{p!\,(|m|+p)!k!\,(|l|+k)!}} \times \begin{cases} \dfrac{icL}{\sigma_z}\Gamma\left(\dfrac{|m|+|l|+2p+2k+1}{2}\right) & m+l \text{ even} \\ R\Gamma\left(\dfrac{|m|+|l|+2p+2k}{2}\right) & m+l \text{ odd} \end{cases} \tag{72}$$

where $\Gamma(x)$ is the gamma function.

5.4 Azimuthal and Radial Mode Coupling

The eigenvalues obtained with Eq. (69) are characterized by two indices, m and p, describing respectively the azimuthal and radial structure of the oscillation mode. In this case, in the limit $N_p \to 0$, the coherent frequencies are still given by Eq. (58), and all the modes with the same m but different p have the same frequency. As we increase N_p slightly, the frequencies shift away from the unperturbed values and the modes shift accordingly. The frequency shifts are initially much smaller than ω_s. Therefore, in this case, radial modes can couple only if they belong to the same azimuthal family with a given m. Therefore, if we focus our attention on the radial modes, for a given m, we can leave only the term $l = m$, thus obtaining

$$\left[\frac{\Omega}{\omega_s} - m\right] a_{mp} = \sum_{k=0}^{\infty} M_{pk}^{mm} a_{mk}. \tag{73}$$

Since the real part of $Z_{||}(\omega)$ is an even function of ω and its imaginary part is uneven, we have that M_{pk}^{mm} is real and $M_{pk}^{mm} = M_{kp}^{mm}$. The matrix M_{pk}^{mm} is then Hermitian. As a consequence, the eigenvalues, i. e. the coherent frequencies, are always real, and radial modes do not couple. If we further increase N_p however, the frequency shifts become comparable to ω_s, so that coupling of azimuthal modes can occur. To simplify the analysis, generally only one radial mode is considered for every azimuthal family. As an example, if we retain only the radial modes with $p = 0$, assumed to be the most prominent, we get

$$\left[\frac{\Omega}{\omega_s} - m\right] a_{m0} = \sum_{l=-\infty}^{\infty} M_{00}^{ml} a_{l0} \tag{74}$$

where the matrix element M_{00}^{ml} is no longer symmetric. In this case we obtain that, above a given value of N_p, two azimuthal modes can couple producing a complex $\Omega^{(m,0)}$ and then an instability. As an example, in Figure 8 we show the coherent frequencies of the

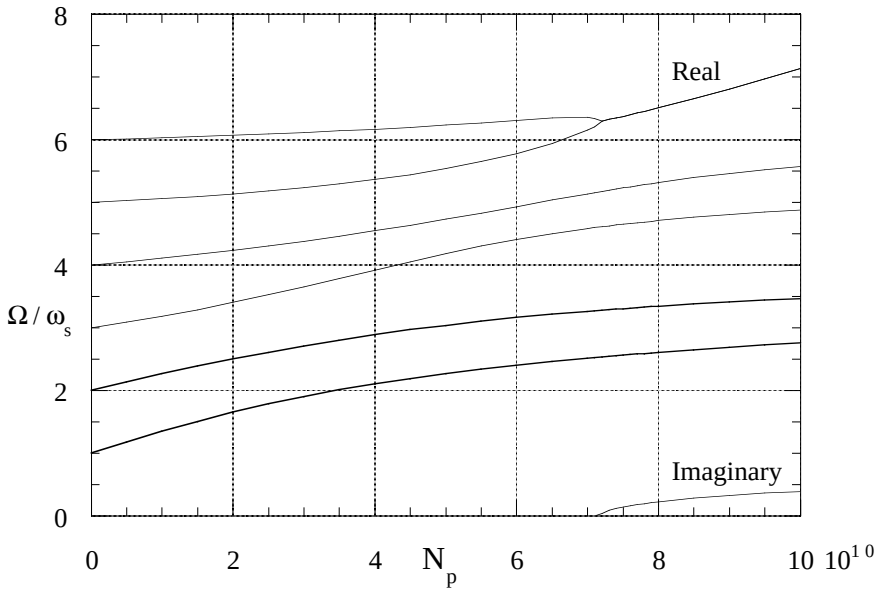

Figure 8: Longitudinal mode frequency Ω/ω_s versus N_p for a pure RL impedance.

first positive modes versus N_p for a pure RL impedance. When N_p reaches the threshold, the modes $m = 5$ and $m = 6$ of the example couple, producing an imaginary component of Ω with values either positive and negative. According to Eq. (54), the negative term is responsible for the instability.

It is worth noting that the threshold obtained with such a method can be much higher than the measured one. The reason is that radial modes with the same azimuthal number can actually couple before a frequency shift of the order of ω_s. Equation (73) cannot predict such behavior because of the symmetry of the bunch distribution. In fact, as we will discuss in the next section, for asymmetric bunches radial mode coupling can occur even if they belong to the same azimuthal family.

5.5 Numerical Solution of the Fokker-Planck Equation

The complete problem of simultaneous accounting for azimuthal and radial modes with a perturbed stationary distribution function is very difficult to treat. There are methods that simplify the approach by using particular bunch distributions, such as the double water bag[15]. With this model we can solve analytically the eigenvalue problem of mode coupling also with an asymmetric bunch shape. For every azimuthal mode there are two radial modes, and it can be demonstrated that the distorted bunch distribution can produce radial mode coupling.

A more general method[16] divides the action variable into n intervals such that $0 = J_0 < J_1 < \cdots < J_n$, and, considers J constant, equal to its average value $\overline{J}_p$, in an interval $\Delta J_p = J_{p+1} - J_p$. Then Eq. (56) gives n equations of the kind $(p = 0, \ldots, n-1)$

$$\left[\Omega - m\omega_s\left(\overline{J}_p\right)\right] R_m\left(\overline{J}_p\right) = \frac{c^2\alpha_c e^2 N_p}{2\pi E_0 L_0 \omega_s\left(\overline{J}_p\right)} \left.\frac{\partial \Psi_0}{\partial J}\right|_{\overline{J}_p} \times \sum_{l=-\infty}^{\infty}\sum_{k=0}^{n} R_l\left(\overline{J}_k\right)\Delta J_k \int_0^{2\pi} \varepsilon\left(\overline{J}_p,\phi\right)\sin\left(m\phi\right)d\phi \times \int_0^{2\pi} \cos\left(l\phi'\right) w_{||}\left[z\left(\overline{J}_k,\phi'\right) - z\left(\overline{J}_p,\phi\right)\right] d\phi'. \quad (75)$$

If we multiply by ΔJ_p we get

$$\left[\Omega - m\omega_s\left(\overline{J}_p\right)\right] R_{mp} = \sum_{l=0}^{\infty}\sum_{k=0}^{n} M_{pk}^{ml} R_{lk} \quad (76)$$

with

$$M_{pk}^{ml} = \frac{c^2\alpha_c e^2 N_p \Delta J_p}{2\pi E_0 L_0 \omega_s\left(\overline{J}_p\right)} \left.\frac{\partial \Psi_0}{\partial J}\right|_{\overline{J}_p} \int_0^{2\pi} \varepsilon\left(\overline{J}_p,\phi\right)\sin\left(m\phi\right)d\phi \times \int_0^{2\pi} \cos\left(l\phi'\right) w_{||}\left[z\left(\overline{J}_k,\phi'\right) - z\left(\overline{J}_p,\phi\right)\right] d\phi' \quad (77)$$

Equation (76) can produce imaginary values of Ω, and thus coupling, even in the case of each azimuthal number m separately analyzed. This method can predict the threshold with better accuracy.

6 Above threshold

6.1 Boussard Criterion

A simple method generally used to obtain a first estimate of the microwave instability threshold is known as the Boussard criterion, and it is derived from the coasting-beam theory applied to the single-bunch case[17]. To justify such an assumption, it can be observed that at high frequencies, in the microwave regime, a bunch can be thought of as a coasting beam, with an average current equal to the single-bunch peak current. With this hypothesis, the criterion fixes the instability of the bunch above the limit

$$\frac{ce^2 N_p \left|Z_{||}\left(n\right)/n\right|}{\left(2\pi\right)^{3/2} E_0 \alpha_c \sigma_z \sigma_\varepsilon^2} \leq 1 \quad (78)$$

where n is a harmonic of the revolution frequency. If N_p is sufficiently high that the left side of Eq. (78) is greater than 1, then the bunch length σ_z and the energy spread σ_ε increase to restore it back to 1.

Equation (78) was derived assuming a bunch with a Gaussian longitudinal distribution. Together with Eq. (38), it allows us to obtain σ_z or σ_ε as a function of N_p above the instability threshold.

The harmonic of the revolution frequency n is generally chosen as

$$n = \frac{L_0}{2\pi\sigma_z}. \tag{79}$$

Long bunches usually interact with the vacuum chamber at low frequencies (below cut-off) where the impedance is pure inductive. In this case we have

$$\frac{Z_{||}(n)}{n} = i\omega_0 L \tag{80}$$

which does not depend on n.

6.2 Chao-Gareyete Scaling Law

A more general scaling law for bunch lengthening above threshold was suggested by Chao and Gareyete[18]. According to their model, the bunch lengthening σ_z is a function of a single parameter ξ, which in turn depends on other machine parameters:

$$\xi = \frac{I\alpha_c}{\nu_s^2 E_0/e}. \tag{81}$$

If we assume a simple power-law behavior for the longitudinal impedance:

$$\left|\frac{Z}{n}\right| = Z_0\omega^{a-1}, \tag{82}$$

then

$$\sigma_z \propto \left(\xi Z_0 R^3\right)^{1/(2+a)}. \tag{83}$$

For instance for the SPEAR case this results in $\sigma_0 \propto \xi^{1/1.32} a = 0.68$, which means $a = -0.68$ corresponding to an impedance decreasing with frequency.

The Boussard model is a particular case of the Chao-Gareyete scaling law for $a = 1$. This corresponds to a constant longitudinal impedance, typical of storage rings with long bunches.

6.3 Numerical Simulations

Numerical simulations are a valid and reliable tool for investigating single-bunch instability. Usually a simulation code models the single bunch as an ensemble of particles obeying the turn-by-turn equations of motion. Assuming a sinusoidal time-dependent RF voltage linearized around the synchrotron particle, we have

$$\begin{aligned} z_i^n &= z_i^{n-1} - L_0 \alpha_c \frac{\varepsilon_i^{n-1}}{E_0}, \\ \varepsilon_i^n &= \varepsilon_i^{n-1} + \frac{2\pi h e \hat{V} \sin(\phi_s)}{L_0} z_i^n + V_w(z_i^n) - D\varepsilon_i^{n-1} + \sigma_{\varepsilon 0} R \sqrt{2D}, \end{aligned} \tag{84}$$

where i refers to the ith particle, and n to the nth turn, L_0 is the machine circumference, $\sigma_{\varepsilon 0}$ the natural energy spread, R a random number from a normal distribution with average 0 and variance 1, and $V_w(z_i^n)$ the voltage produced by the self-induced short-range wakefields.

Since it is impossible to simulate the motion of 10^{10} to 10^{12} particles for hundreds of thousands of turns, a smaller number of macro-particles, each one representing 10^6 or more particles, is used in the simulations. The number of macro-particles N_m must be high enough to limit the numerical noise, which scales as $1/\sqrt{N_m}$.

The voltage of the self-induced wakefields depends on the single-bunch distribution function according to the relation

$$V_w(z) = eN_p \int_{-\infty}^{\infty} w_{||}(z' - z)\, dz' \int_{-\infty}^{\infty} \Psi(z', \varepsilon) d\varepsilon \tag{85}$$

where N_p is the number of particles per bunch. In our discrete model, we consider the N_m macro-particles distributed in N_{bin} bins, and therefore the induced voltage can be written as

$$V_w(z_i^n) = e \frac{N_p}{N_m} \sum_{z_k > z_i^n}^{k=1,N_{bin}} N_b(z_k)\, w_{||}(z_k - z_i^n) \tag{86}$$

with z_k the coordinate of the kth bin center, and $N_b(z_k)$ the number of macro-particles in the bin.

This method of tracking the bunch particles has been successfully used in bunch lengthening simulations[19] for the SLC[20] damping rings, SPEAR[21], LEP[22], and DAΦNE[23]. In Figure 9 we show an example of the results obtained with the numerical simulations: two distributions of an unstable bunch and the bunch length as function of current.

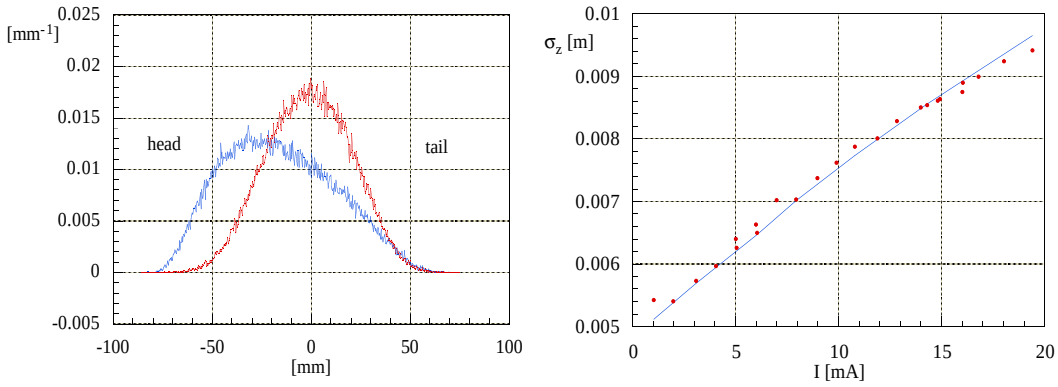

Figure 9: Example of numerical simulations.

References

[1] L. Palumbo, *et al.*, CERN 95-06 (1995).

[2] V. G. Vaccaro, CERN ISR-RF/66-35 (1966).

[3] M. Zobov, *et al.*, KEK Proceedings 96-6, 110 (1996).

[4] R. Klatt, *et al.*, SLAC Report 303 (1986).

[5] Y. H. Chin, LBL Report 35258, UC-414 (1994).

[6] A. Hofmann, *et al.*, CERN LEP Note 169 (1979).

[7] See, for example, S. Heifets, Frascati Physics Series **10**, 139 (1998).

[8] K. Bane, SLAC PUB 4618 (1988).

[9] A. Chao, Physics of Collective Beam Instabilities in High Energy Accelerators, Wiley Interscience (1993).

[10] C. Bernardini, *et al.*, LNF Internal Note 34 (1960).

[11] J. Haissinski, Il Nuovo Cimento **18B**, (1), 72 (1973).

[12] F. Sacherer, CERN/SI-BR/72-5 (1972).

[13] B. Zotter, CERN-SPS/81-18,19,20 (DI) (1981).

[14] J. L. Laclare, CERN 87-03, Vol I (1987).

[15] A. Chao, *et al.*, Proc of the 1995 PAC, Dallas (1995).

[16] K. Oide, *et al.*, KEK Preprint 90-10 (1990).

[17] D. Boussard, CERN-LABII/RF/INT75-2 (1975).

[18] A. Chao, *et al.*, Particle Accelerators **25**, 229 (1990).

[19] A. Renieri, LNF - 75 / 11 (R) Frascati (1976).

[20] K. L. F. Bane, *et al.*, Proc of the 1993 PAC, Washington D.C., 3339 (1993).

[21] R. Sieman, NIM **203**, 57 (1982).

[22] T. Weiland, DESY 81-088 (1981).

[23] M. Zobov, *et al.*, DAΦNE Technical Note BM-3, Frascati (1998).

APPENDIX A

Derivation of Fokker-Planck Equation

To obtain the Fokker-Planck equation, we first substitute Eq. (23) into the distribution function $\Psi\left[z\left(t-T_0\right);\varepsilon\left(t-T_0\right);t-T_0\right]$ and then take a time linear expansion of such a function:

$$\Psi\left[z\left(t\right)+\frac{\partial H}{\partial\varepsilon}T_0,\varepsilon\left(t\right)-\frac{\partial H}{\partial z}T_0+D\varepsilon+\frac{R\left(T_0\right)}{E_0};t-T_0\right]$$
$$=\Psi\left[z\left(t\right)+\frac{\partial H}{\partial\varepsilon}T_0,\varepsilon\left(t\right)-\frac{\partial H}{\partial z}T_0+D\varepsilon+\frac{R\left(T_0\right)}{E_0};t\right]-\frac{\partial\Psi}{\partial t}T_0 \quad (87)$$

where the time derivative of Ψ is evaluated at point $z\left(t\right),\varepsilon\left(t\right)$.

If we now expand the first term in the right side of Eq. (87), we obtain

$$\Psi\left[z\left(t\right)+\frac{\partial H}{\partial\varepsilon}T_0,\varepsilon\left(t\right)-\frac{\partial H}{\partial z}T_0+D\varepsilon+\frac{R\left(T_0\right)}{E_0};t\right]$$
$$=\Psi\left[z\left(t\right)+\frac{\partial H}{\partial\varepsilon}T_0,\varepsilon\left(t\right)-\frac{\partial H}{\partial z}T_0+D\varepsilon;t\right]+$$
$$\frac{\partial\Psi}{\partial\varepsilon}\frac{R\left(T_0\right)}{E_0}+\frac{1}{2}\frac{\partial^2\Psi}{\partial\varepsilon^2}\frac{R^2\left(T_0\right)}{E_0^2}+\sum_{n=3}^{\infty}\frac{1}{n!}\frac{\partial^n\Psi}{\partial\varepsilon^n}\frac{R^n\left(T_0\right)}{E_0^n}. \quad (88)$$

Before integrating the right side of Eq. (24), we write

$$\int_{-\infty}^{\infty}R^n\left(T_0\right)P\left[R\left(T_0\right)\right]dR\left(T_0\right)=\overline{R^n\left(T_0\right)}. \quad (89)$$

Because of the definition of probability density, we have $\overline{R^0(T_0)} = 1$, and, since $R(T_0)$ has a zero average value, then $\overline{R^1(T_0)} = 0$. We can now integrate the right side of Eq. (24) by using Eqs. (87) and (88), thus obtaining

$$\Psi[z(t),\varepsilon(t);t]\,dzd\varepsilon| = \left\{\Psi\left[z(t)+\frac{\partial H}{\partial\varepsilon}T_0,\varepsilon(t)-\frac{\partial H}{\partial z}T_0+D\varepsilon;t\right]-\right.$$
$$\left.\frac{\partial\Psi}{\partial t}T_0+\frac{1}{2}\frac{\partial^2\Psi}{\partial\varepsilon^2}\frac{\overline{R^2(T_0)}}{E_0^2}+\sum_{n=3}^{\infty}\frac{1}{n!}\frac{\partial^n\Psi}{\partial\varepsilon^n}\frac{\overline{R^n(T_0)}}{E_0^n}\right\}dzd\varepsilon|_{t-T_0}. \quad (90)$$

The next step is to expand the distribution function in the right side of Eq. (90) around the point (z,ε), again keeping only first-order terms in time:

$$\Psi\left[z(t)+\frac{\partial H}{\partial\varepsilon}T_0,\varepsilon(t)-\frac{\partial H}{\partial z}T_0+D\varepsilon;t\right]$$
$$=\Psi[z(t),\varepsilon(t);t]+\frac{\partial\Psi}{\partial z}\frac{\partial H}{\partial\varepsilon}T_0+\frac{\partial\Psi}{\partial\varepsilon}\left(-\frac{\partial H}{\partial z}T_0+D\varepsilon\right). \quad (91)$$

By introducing Eq. (91) into Eq. (90) and by using the relations (20), still ignoring second-order terms in time, we finally get

$$\frac{\partial\Psi}{\partial t}=\frac{\partial\Psi}{\partial z}\frac{\partial H}{\partial\varepsilon}-\frac{\partial\Psi}{\partial\varepsilon}\frac{\partial H}{\partial z}+\frac{D}{T_0}\left(\Psi+\varepsilon\frac{\partial\Psi}{\partial\varepsilon}\right)+\frac{1}{2}\frac{\partial^2\Psi}{\partial\varepsilon^2}\frac{\overline{R^2(T_0)}}{T_0E_0^2} \quad (92)$$

where we have neglected the higher-order terms:

$$\sum_{n=3}^{\infty}\frac{1}{n!}\frac{\partial^n\Psi}{\partial\varepsilon^n}\frac{\overline{R^n(T_0)}}{T_0E_0^n}. \quad (93)$$

APPENDIX B

Solution of Haissinski Equation for Pure Resistive Impedance

Applying the logarithm derivative on both sides of Eq. (40), we get

$$\frac{\rho_0'(z)}{\rho_0(z)}=-\frac{z}{\sigma_{z0}^2}+\frac{e^2N_pcR}{L_0E_0\alpha_c\sigma_{\varepsilon0}^2}\rho_0(z) \quad (94)$$

which is a Bernoulli differential equation, the general solution of which is

$$\rho_0(z)=\frac{\exp[-U_0(z)]}{k-\xi_1\int_0^z\exp[-U_0(x)]\,dx} \quad (95)$$

with

$$U_0(z)=\int_0^z\frac{x}{\sigma_{z0}^2}dx=\frac{z^2}{2\sigma_{z0}^2} \quad (96)$$

and

$$\xi_1 = \frac{e^2 N_p c R}{L_0 E_0 \alpha_c \sigma_{\varepsilon 0}^2}. \tag{97}$$

The constant k is obtained by the normalization condition (3). If we use an auxiliary function $f(z)$ such that

$$f(z) = k - \xi_1 \int_0^z \exp\left[-U_0(x)\right] dx \tag{98}$$

then

$$\exp\left[-U_0(z)\right] = -\frac{f'(z)}{\xi_1}. \tag{99}$$

The normalization condition with such a function gives

$$\int_{-\infty}^{\infty} \frac{f'(z)}{f(z)} dz = -\xi_1 \tag{100}$$

which we can integrate, obtaining

$$\ln\left[f(z)\right]\Big|_{-\infty}^{\infty} = \ln\left[\frac{k - \xi_1 \int_0^{\infty} \exp\left[-U_0(x)\right] dx}{k - \xi_1 \int_0^{-\infty} \exp\left[-U_0(x)\right] dx}\right] = -\xi_1. \tag{101}$$

By solving the above equation with respect to k we get

$$k = \sqrt{\frac{\pi}{2}} \xi_1 \sigma_{z0} \frac{1 + e^{-\xi_1}}{1 - e^{-\xi_1}} = \sqrt{\frac{\pi}{2}} \xi_1 \sigma_{z0} \coth\left(\frac{\xi_1}{2}\right) \tag{102}$$

and then we can write the distribution function as

$$\rho_0(z) = \frac{\exp\left(-\dfrac{z^2}{2\sigma_{z0}^2}\right)}{\xi_1 \sigma_{z0} \sqrt{\dfrac{\pi}{2}} \left[\coth\left(\dfrac{\xi_1}{2}\right) - \operatorname{erf}\left(\dfrac{z}{\sqrt{2}\sigma_{z0}}\right)\right]} \tag{103}$$

for which we have used the definition of error function

$$\operatorname{erf}(x) = \frac{2}{\sqrt{\pi}} \int_0^z \exp\left(-x^2\right) dx. \tag{104}$$

APPENDIX C

Derivation of Linearized Vlasov Equation

If we ignore the second-order infinitesimal

$$\frac{\partial \Psi_1}{\partial \varepsilon} \frac{\partial H_1}{\partial z} \cong 0 \tag{105}$$

and the effects of radiation damping and fluctuation noise on the perturbation function Ψ_1, we get

$$\frac{\partial \Psi_1}{\partial t} = \frac{\partial \Psi_1}{\partial z}\frac{\partial H_0}{\partial \varepsilon} - \frac{\partial \Psi_0}{\partial \varepsilon}\frac{\partial H_1}{\partial z} - \frac{\partial \Psi_1}{\partial \varepsilon}\frac{\partial H_0}{\partial z}. \tag{106}$$

It is convenient, at this point, to introduce the two action angle variables, J and ϕ, defined as

$$\begin{aligned} J(H) &= \frac{1}{2\pi}\oint_{-\text{motion}} \varepsilon dz = \frac{1}{\pi}\int_{z_{\min}}^{z_{\max}} \left(\frac{2H}{c\alpha_c} - \frac{2\varphi(z)}{\alpha_c^2 E_0}\right)^{\frac{1}{2}} dz, \\ \dot{\phi} &= \omega_s(J) = \frac{\partial H}{\partial J}, \end{aligned} \tag{107}$$

where the line integral is extended to a whole period of motion, and is opposite to the direction described by a particle in the phase space, in order to have a positive value of the action variable J. The values of $z_{\min}$ and $z_{\max}$ depend on the Hamiltonian H. One property of J is that it is a function only of the Hamiltonian, and it is proportional to the region, in the phase space, enclosed by the trajectory. It is therefore a constant of the motion for a conservative system. Furthermore, the stationary distribution Ψ_0 depends only on J and not on ϕ.

With the introduction of the generating functions related to the Legendre transformations, it is possible to demonstrate that

$$\begin{aligned} \frac{\partial J}{\partial z} &= \frac{\partial \varepsilon}{\partial \phi}, \\ \frac{\partial J}{\partial \varepsilon} &= -\frac{\partial z}{\partial \phi}. \end{aligned} \tag{108}$$

The above definitions allow us to write Eq. (106) in a more compact form. In fact we have

$$\begin{aligned} \frac{\partial H_0}{\partial \varepsilon} &= \frac{\partial H_0}{\partial J}\frac{\partial J}{\partial \varepsilon} = -\omega_s(J)\frac{\partial z}{\partial \phi}, \\ \frac{\partial H_0}{\partial z} &= \frac{\partial H_0}{\partial J}\frac{\partial J}{\partial z} = \omega_s(J)\frac{\partial \varepsilon}{\partial \phi}, \end{aligned} \tag{109}$$

and then Eq. (106) becomes

$$\frac{\partial \Psi_1}{\partial t} = -\frac{\partial \Psi_0}{\partial \varepsilon}\frac{\partial H_1}{\partial z} - \omega_s(J)\left(\frac{\partial \Psi_1}{\partial z}\frac{\partial z}{\partial \phi} + \frac{\partial \Psi_1}{\partial \varepsilon}\frac{\partial \varepsilon}{\partial \phi}\right). \tag{110}$$

The term in parentheses is just the derivative of Ψ_1 with respect to ϕ, and the first term on the right side can be written as

$$\frac{\partial \Psi_0}{\partial \varepsilon}\frac{\partial H_1}{\partial z} = \frac{\partial \Psi_0}{\partial J}\frac{\partial J}{\partial \varepsilon}\frac{\partial H_1}{\partial z} = \frac{1}{\omega_s(J)}\frac{\partial H_0}{\partial \varepsilon}\frac{\partial \Psi_0}{\partial J}\frac{\partial H_1}{\partial z} \tag{111}$$

since Ψ_0 is independent of ϕ. If we now use the definition of Hamiltonian (15) and Eq. (50), we have

$$\frac{\partial \Psi_0}{\partial \varepsilon}\frac{\partial H_1}{\partial z} = -\frac{c^2 \alpha_c e^2 N_p \varepsilon}{E_0 L_0 \omega_s (J)}\frac{\partial \Psi_0}{\partial J}\int_{-\infty}^{\infty} \rho_1 (z';t)\, w_{||} (z'-z)\, dz' \tag{112}$$

which, introduced in Eq. (110), gives finally

$$\frac{\partial \Psi_1}{\partial t} = -\omega_s (J)\frac{\partial \Psi_1}{\partial \phi} + \frac{c^2 \alpha_c e^2 N_p}{E_0 L_0 \omega_s (J)}\frac{\partial \Psi_0}{\partial J}\varepsilon \int_{-\infty}^{\infty} \rho_1 (z';t)\, w_{||} (z'-z)\, dz'. \tag{113}$$

APPENDIX D

Matrix Elements for Gaussian and Parabolic Distributions

In terms of action-angle variables, the stationary Gaussian distribution function Eq. (29) can be written as

$$\Psi_0 (J) = \overline{\Psi} \exp\left[-\frac{\omega_s J}{\overline{H}}\right]. \tag{114}$$

The constant $\overline{\Psi}$, obtained with the normalization condition (21), is

$$\overline{\Psi} = \frac{\omega_s}{2\pi \overline{H}} \tag{115}$$

and then

$$\Psi_0 (J) = \overline{\Psi} \exp\left[-2\pi \overline{\Psi} J\right] \tag{116}$$

with which the weight function becomes

$$w (J) = 2\pi \overline{\Psi} \exp\left[-2\pi \overline{\Psi} J\right]. \tag{117}$$

The normalization condition on the polynomials is therefore

$$2\pi \overline{\Psi} \int_0^{\infty} \exp\left[-2\pi \overline{\Psi} J\right] f_{|m|k} (J)\, f_{|m|l} (J)\, dJ = \delta_{kl}. \tag{118}$$

The polynomials that satisfy such a relation are the generalized Laguerre polynomials $L_l^{(|m|)}$ for which we have

$$\sqrt{\frac{l!k!}{(|m|+l)!\,(|m|+k)!}} \int_0^{\infty} x^{|m|} L_l^{(|m|)} (x)\, L_k^{(|m|)} (x)\, e^{-x} dx = \delta_{kl}, \tag{119}$$

which, compared with Eq. (118), allows us to conclude that

$$f_{|m|l} (J) = \sqrt{\frac{l!}{(|m|+l)!}} \left(2\pi \overline{\Psi} J\right)^{\frac{|m|}{2}} L_l^{(|m|)} \left(2\pi \overline{\Psi} J\right) \tag{120}$$

and, therefore, the matrix elements (70) become

$$M_{pk}^{ml} = -i\frac{mc^2e^2N_p\overline{\Psi}}{\omega_s E_0 L_0} i^{l-m}\sqrt{\frac{p!k!}{(|m|+p)!\,(|l|+k)!}}\int_{-\infty}^{\infty}\frac{Z_{||}(\omega)}{\omega}d\omega$$
$$\times\int_0^{\infty} x^{\frac{|m|}{2}}e^{-x}L_p^{(|m|)}(x)\,J_m\left(\omega\sqrt{\frac{\alpha_c x}{\pi\overline{\Psi}c\omega_s}}\right)dx$$
$$\times\int_0^{\infty} y^{\frac{|l|}{2}}e^{-y}L_k^{(|l|)}(y)\,J_l\left(\omega\sqrt{\frac{\alpha_c y}{\pi\overline{\Psi}c\omega_s}}\right)dy. \quad (121)$$

The last two integrals can be solved; in fact we have

$$\int_0^{\infty} x^{\frac{|m|}{2}}e^{-x}L_p^{(|m|)}(x)\,J_m\left(a\sqrt{x}\right)dx = S(m)\,\frac{1}{p!}\left(\frac{a}{2}\right)^{|m|+2p}\exp\left[-\frac{a^2}{4}\right] \quad (122)$$

where

$$S(m) = \begin{cases}(-1)^m & \text{if } m<0\\ 1 & \text{if } m\geq 0\end{cases} \quad (123)$$

and then

$$M_{pk}^{ml} = -i\frac{c^2e^2N_p\overline{\Psi}}{\omega_s E_0 L_0} i^{|l|-|m|}\frac{m}{\sqrt{p!\,(|m|+p)!k!\,(|l|+k)!}}$$
$$\times\int_{-\infty}^{\infty}\frac{Z_{||}(\omega)}{\omega}\left(\frac{\omega}{2}\sqrt{\frac{\alpha_c}{\pi\overline{\Psi}c\omega_s}}\right)^{|m|+|l|+2p+2k}\exp\left[-\frac{\omega^2\alpha_c}{2\pi\overline{\Psi}c\omega_s}\right]d\omega, \quad (124)$$

which, in terms of bunch length σ_z and natural energy spread $\sigma_{\varepsilon 0}$, due to the relation

$$2\pi\overline{\Psi} = \frac{1}{\sigma_z\sigma_{\varepsilon 0}}, \quad (125)$$

can also be written as

$$M_{pk}^{ml} = -i\frac{c^2e^2N_p}{2\pi\omega_s E_0 L_0\sigma_z\sigma_{\varepsilon 0}} i^{|l|-|m|}\frac{m}{\sqrt{p!\,(|m|+p)!k!\,(|l|+k)!}}$$
$$\times\int_{-\infty}^{\infty}\frac{Z_{||}(\omega)}{\omega}\left(\frac{\omega\sigma_z}{\sqrt{2}c}\right)^{|m|+|l|+2p+2k}\exp\left[-\frac{\omega^2\sigma_z^2}{c^2}\right]d\omega. \quad (126)$$

The same procedure for the case of a parabolic bunch distribution leads to

$$f_{|m|l}(J) = \sqrt{\frac{2\,(m+2l+1/2)\,l!\Gamma(m+l+1/2)}{(m+l)!\Gamma(l+1/2)}}$$
$$\times\left(\frac{J}{J_{max}}\right)^{m/2}P_l^{m,-1/2}\left(1-2\frac{J}{J_{max}}\right) \quad (127)$$

with $P_l^{m,-1/2}$ the Jacobi polynomials and

$$M_{pk}^{ml} = -i\frac{3c^2e^2N_p}{2\pi\omega_s E_0 L_0 z_{max}^2} i^{|l|-|m|} m \sqrt{\frac{(m+2p+1/2)\,\Gamma\left(m+p+1/2\right)\Gamma\left(p+1/2\right)}{p!\,(m+p)!}} \times \sqrt{\frac{(l+2k+1/2)\,\Gamma\left(l+k+1/2\right)\Gamma\left(k+1/2\right)}{k!\,(l+k)!}} \times \int_{-\infty}^{\infty} \frac{Z_{||}\left(\omega\right)}{\omega} \frac{J_{m+2p+1/2}\left(\frac{\omega}{c}z_{max}\right) J_{l+2k+1/2}\left(\frac{\omega}{c}z_{max}\right)}{\frac{\omega}{c}z_{max}} d\omega. \quad (128)$$